Review of Scientific Instruments

A modification of Ångström's method that employs photothermal radiometry to measure thermal diffusivity: Application to chemical vapor deposited diamond

Cite as: Review of Scientific Instruments **69**, 237 (1998); https://doi.org/10.1063/1.1148873
Submitted: 25 July 1997 . Accepted: 20 October 1997 . Published Online: 04 June 1998

A. Feldman, and N. M. Balzaretti

A modification of Ångström's method that employs photothermal radiometry to measure thermal diffusivity: Application to chemical vapor deposited diamond

A. Feldman[a] and N. M. Balzaretti[b]
National Institute of Standards and Technology, Gaithersburg, Maryland 20899

(Received 25 July 1997; accepted for publication 20 October 1997)

A modification of the one dimensional Ångström's method that employs photothermal radiometry has been used to determine the longitudinal thermal diffusivity of three thin long bars of chemical vapor deposited diamond. Long bar specimens permit us to use a simple one-dimensional treatment that employs a linear least squares fitting procedure on both magnitude and phase data as a function of position, provided that the condition for ignoring end effects is fulfilled. Any differences in diffusivities obtained from magnitude data and from phase data can be attributed to surface heat losses; the values of diffusivity obtained with the two types of data showed no significant difference. The diffusivities obtained agree reasonably well with the mean values calculated from measurements made by several other laboratories on the same specimens. The heat source was the beam of an argon-ion laser focused onto the specimen surface either with a cylindrical lens to form a line focus or with a spherical lens to form a point focus. The differences in diffusivities obtained when a line source was used and when a point source was used were not statistically significant. A theoretical calculation indicates that the measurements on the specimen were made sufficiently far from the heat source for the one-dimensional treatment to be valid whether the line source or the point source were used: either source is expected to give the same result as was observed experimentally. A point source is preferable because the optical configuration of the experiment is simpler and larger signals are obtainable.
[S0034-6748(98)04101-X]

I. INTRODUCTION

In this article, we present an experimental procedure that employs photothermal radiometry[1] (PTR) in combination with the one dimensional geometry employed by Ångström[2] to measure longitudinal thermal diffusivity, with application to chemical vapor deposited (CVD) diamond. PTR is a technique that has been used to determine the thermal diffusivity of various materials[3–7] and in particular CVD diamond.[8–12] The technique is based on the detection of thermal radiation emitted from a specimen that has been heated by a modulated source,[4–8,11,12] usually a chopped laser beam, or a pulsed source,[3,9,10] such as pulsed laser beam. We limit our treatment here to the ac case. The thermal diffusivity, D, can be obtained from the behavior of the thermal signal either as a function of the modulation angular frequency,[4,5,7,8,12] ω, or as a function of the distance, z, from the heated spot.[6,11] The signal will consist of both a magnitude and a phase. In order to determine D for a given specimen geometry, one must fit the experimentally measured phase and/or magnitude to theoretical models that predict the complex temperature dependence on ω and/or z. The theoretical and numerical analysis required for obtaining D are one of the challenges of the PTR technique for arbitrary specimen shapes and heating beam geometries.

By choosing a specimen in the shape of a long thin bar, considerable simplification of the analysis occurs. If the specimen is sufficiently long, ω can be made sufficiently large so that end effects will be minimized, yet sufficiently small so that the temperature distribution along the width and thickness of the specimen can be considered uniform, even if the heating source is nonuniform. Thus, the following simple one dimensional steady state solution of the thermal diffusion equation is applicable:

$$T(z)=\frac{q}{2\sqrt{\omega\kappa\rho C}}\,e^{-\frac{|z|}{\mu}+\frac{|z|}{\mu}i+\frac{\pi}{4}i}, \tag{1}$$

where z is the distance along the bar from a heating source near the center of the bar, $T(z)$ is the complex temperature, q is the power input, κ is the thermal conductivity, ρ is the density, C is the specific heat, and μ is the thermal diffusion length given by $\mu=\sqrt{2D/\omega}$; this one dimensional case was treated by Ångström[2] and any method based on it is called Ångström's method or a modified Ångström method. Both the phase of $T(z)$, $\varphi(z)$, and the logarithm of the magnitude, $\ln|T(z)|$, depend linearly on z provided the region of measurement is sufficient far from the heating source; thus, the calculation of D from the experimentally measured phase and magnitude as a function of z is straightforward. Fabbri and Fenici[6] have shown only that phase of a thermal signal versus radial distance from an ac heating source will be linear provided the region of measurement is sufficiently far from the source. In an appendix, we give the general solution to heating of a thin bar by a nonuniform heating source and show that under the condition describe in this article, the

[a]Electronic mail: albert.feldman@nist.gov
[b]Permanent address: Instituto de Fisica, UFRGS, Porto Alegre, RS-91501-970, Brazil.

measurements have been performed sufficiently far from the heating source to insure that Eq. (1) is appropriate for the analysis of both phase and magnitude data.

Hatta *et al.*[13] used a one-dimensional approach to measure the thermal diffusivity of long bars. In their procedure, a partially masked specimen was illuminated with a modulated halogen lamp and a thermocouple was attached to the specimen in the shadowed region beneath the mask. While moving the mask parallel to the specimen surface along the length of the bar, they monitored the temperature as a function of the distance from the thermocouple to the shadow edge which was perpendicular to the long specimen dimension. Gu and Hatta[14] have modified Hatta's original technique[13] by heating a narrow strip across the specimen rather than a large area of the specimen.

Altmann *et al.*[15] have employed another modification of Ångström's method. They deposit a metallic heating strip on the specimen and measure the phase of the thermal signal versus position with a thermocouple that is held in contact with the specimen surface at different distances from the heating source. The magnitude is not used because it will depend on the reproducibility of the heat transfer between the thermocouple and the specimen at different contact points whereas the phase is not expected to be as sensitive to this heat transfer.

In this work, we present results for D calculated from PTR experimental data obtained by a modification of Ångström's method where we used an infrared detector instead of thermocouples to monitor the phase and magnitude of the thermal signal as a function of the distance from the heated region. The specimens were three free-standing bars of CVD diamond. The heat source was the beam of an argon-ion laser focused onto a specimen surface either with a cylindrical lens to form a line focus along the specimen width or with a spherical lens to form point focus centered on the specimen width. The differences in diffusivities obtained when a line source was used and when a point source was used were not statistically significant. Larger signals were obtainable with a point heating source because more power could be put into the specimen.

To verify the validity of the approach used, our results are compared to previous results obtained on these same specimens by different experimental techniques.[16] In order to make the comparison meaningful, our results are compared only with those based on Ångström's method. Finally, we give values for thermal conductivity, κ, of the specimens based on the relationship $\kappa=\rho CD$.

Advantages of the use of the PTR technique include: (1) it is a noncontact method; (2) it can use higher modulation frequencies than techniques that use thermocouples. The advantages of the long bar geometry is that a linear fit can be used both with the magnitude and phase of the thermal signal to compute D. Although planar geometries require less specimen preparation, the linear theory is applicable only to the phase;[6] a nonlinear fitting procedure is needed if the magnitude is to be used in the computation. Furthermore, the long bar geometry confines the thermal energy to a smaller region than a planar geometry region resulting a larger thermal signal.

II. THEORETICAL CONSIDERATIONS

The homogeneous heat diffusion equation for one-dimensional heat flow is given by[4,10]

$$\frac{d^2T(z)}{dz^2}+\left(\frac{\omega}{D}\,i-h\right)T(z)=0, \tag{2}$$

where h is a term that accounts for heat loss to the surroundings, such as radiation loss. Heat input is treated as a boundary condition with a time dependence, $qe^{-i\omega t}$. Equation (1) represents a simple solution to Eq. (2). Hatta *et al.*[17] and Gu and Hatta[14] have discussed the range of validity of Eq. (1) based on specimen dimensions. In the strictest sense, it is valid under the following conditions: heating occurs uniformly in a plane normal to the bar axis; heat losses to the surroundings are negligible at the measurement frequency ($h=0$); and, z is sufficiently far from the ends of the specimen so that reflections of thermal waves from the ends are negligible. The distance from an end should be $>1.5\,\mu$. The solution may still be valid even if these conditions do not strictly hold. If the specimen is heated on the top surface with a line source, Eq. (1) is valid when the thickness of the bar, $d\ll\mu$ provided the measurement is made several times d away from the heating source. If the specimen is heated with a point source on a surface, we must add the condition that half the specimen width, $w/2\ll\mu$. Even the conditions on the on w and d can be relaxed considerably, provided that the data points used in computations are sufficiently far from the heating source. In the appendix, we present the three dimensional solution to the thermal diffusion equation for a long rectangular bar assuming a nonuniform heat source. We show the validity of Eq. (1) under the experimental conditions described in this article.

When conditions for satisfying Eq. (1) are met, then $\ln|T(z)|$ and $\varphi(z)=-\arctan(\Im T/\Re T)$ are linear functions of z with the magnitude of the slope equal to $1/\mu$, where $\Im T$ is the imaginary part of T and $\Re T$ is the real part of T. Thus, by determining these slopes from the experimental data, we can compute μ and, hence, D.

If heat loss to the surroundings is present ($h\neq 0$) the solution to Eq. (2) will be modified.[2,18] Both $\ln|T(z)|$ and $\varphi(z)$ will still depend linearly on z, but, their slopes will differ. However, the product of the slopes will be $1/\mu^2$ so we can still compute D. This provides a test for heat loss to the surroundings at the measurement frequency; if the slope of $\ln|T(z)|$ is steeper than the slope of $\varphi(z)$, then significant heat loss is present. An examination of Eq. (2) indicates that the importance of h decreases with increasing ω.[19]

III. EXPERIMENTAL METHOD

The specimens, which were long thin bars of CVD diamond, are described in Table I. During the experiment, a specimen was held at one end by double sided adhesive tape. The center portion and the free end of the specimen were unsupported so that both the back and front surfaces were in contact with air. A chopped argon laser beam (514.5 nm) operating at a power of ~ 1.0 W, was used to heat the specimen at the approximate center of the front surface. The amount of energy reaching the specimen was about 20% of

TABLE I. CVD diamond specimens.

Designations	Dimensions (mm) length	width, w	thickness, d	Description
LB-E	40	4	0.30	dark
LB-T	50	4	0.40	translucent
LB-X	50	4	0.35	transparent

the laser power due to chopping of the laser radiation and reflection and absorption by the optical elements. Figure 1 shows the experimental setup used.[20]

The heating beam that was focused onto the specimen was assumed to have a gaussian intensity profile and the beam diameter, as determined from the $1/e$ points, was calculated from a knife-edge test. Two different heating configuration were used: in one case, the heating beam was focused to a pointlike image with a gaussian beam diameter of about 0.044 mm; in the other case, a cylindrical focusing lens was used to produce an elongated linelike image. The beam was assumed to have an anisotropic gaussian profile; the full length between the $1/e$ points was 3.6 mm and the full width between the $1/e$ points was 0.2 mm. The long dimension of the beam was perpendicular to the long axis of the specimen. The reason for the two configurations was to determined whether the measurement was sensitive to the shape of the heating beam.

The infrared detector which was made of indium antimonide was located in a cryostat and cooled by liquid nitrogen. Its sensitive area was 1 mm in diameter. The infrared radiation emitted by the specimen was focused onto the detector by a calcium fluoride lens with a magnification of one. The detector and lens were scanned in a step-wise manner under microcomputer control in steps of 0.5 mm parallel to the specimen surface and along the long specimen dimension. At each detector position, the magnitude and phase of the thermal signal arising from infrared emission was measured by a lock-in amplifier also under microcomputer control and saved to disk. Each data set was obtained at one modulation frequency. The procedure was repeated at different modulation frequencies to improve the accuracy of the results.

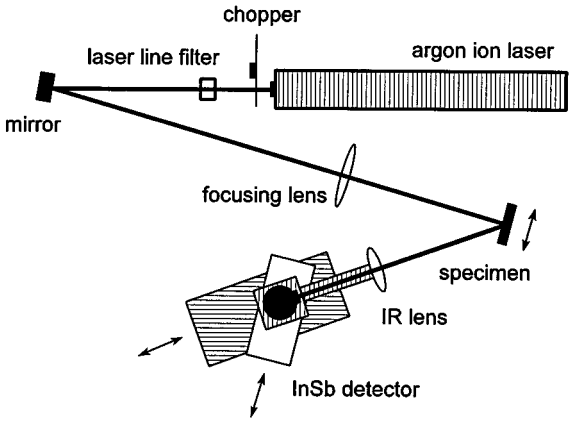

FIG. 1. Schematic diagram of photothermal radiometry experiment. The detector and infrared focusing lens move together, parallel to the specimen surface. The arrows indicate motion of translation stages.

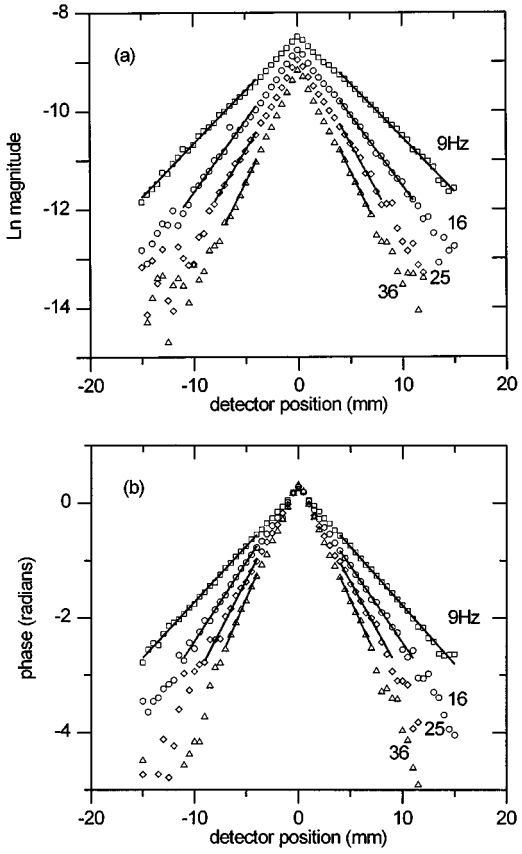

FIG. 2. Typical experimental data for a long bar specimen obtained with the line heat source. The data are from specimen LB-T. Plotted are (a) the logarithm of the signal magnitude vs detector position z and (b) the phase of the signal vs detector position z. Superimposed on the data are straight line segments representing the fits to the data; the extent of the lines represent the region fitted. The modulation frequencies are shown.

Before each measurement, specimen temperature was allowed to stabilize and then the temperature was recorded. The temperature was measured with a type K thermocouple placed in contact with the specimen on the back surface approximately midway between the heated region and a specimen end. The temperature did not vary significantly during one measurement.

In the case of the transparent specimen, LB-X, in order to increase the absorption of the laser energy and, hence, increase the thermal radiation emitted by the specimen, a narrow black stripe of about 1 mm wide was written with a pen marker in the heated spot region of the top surface. The other specimens were not coated because they absorbed sufficient energy for making the measurements.

IV. RESULTS AND DISCUSSION

Figure 2 shows the experimental data for specimen LB-T obtained with the line heat source; a similar set of data was obtained with the point heat source. Measurements were made at modulation frequencies (f) of 9, 16, 25, and 36 Hz. In addition to the experimental data points on the figure, we show straight line segments representing linear fits to the data. The extent of the segments indicates the range of the

TABLE II. Average specimen thermal diffusivity and thermal conductivity.[a]

Specimen designation	D ($cm^2\ s^{-1}$) Point source	T_{ave}(°C)	Line source[a]	T_{ave}(°C)	Line source[b]	T_{ave}(°C)	κ ($W\ cm^{-1}\ K^{-1}$)
LB-E	2.2±0.1	29.0±0.5	2.0±0.2	30.8±0.5	2.2±0.2	29.2±0.1	3.9±0.4
LB-T	6.6±0.4	31.5±0.6	6.3±0.6	30.5±0.7	6.4±0.6	30.9±1.0	12±1
LB-X	7.9±0.9	28.8±0.2	7.9±0.6	30.3±0.8	8.0±0.8	27.5±0.4	14±1

[a]All combined standard uncertainties (±) are attributed principally to measurement repeatability and thus are taken to be one standard deviation of a measurement.
[b]T_{ave}=average specimen temperature.

data used in the computation. The range of fit was chosen to maintain the applicability of Eq. (1) to the analysis, namely, all of the data are sufficiently far from the specimen ends and from the heating source to insure that $\ln|T(z)|$ and $\varphi(z)$ depend linearly on z. Similar analyses were done for the other two specimens, both for data obtained with the line source and data obtained with the point source. For a given heat source geometry and frequency, we calculated four values for the slope, corresponding to the right and left side of the heated spot from both the magnitude data and the phase data. Therefore, from data for the four frequencies, we obtained 16 values for the slope. The average of these 16 values was used to compute D; the combined standard uncertainties[21] are attributed principally to measurement repeatability and thus are taken to be one standard deviation of a measurement.

Table II lists the values of thermal diffusivity obtained together with the average specimen temperature. Three values of D are given for each specimen, one value based on one point source measurement set and two values based on two line source measurement sets. We performed the measurements with the line source twice in order to check the reproducibility of the results. These are labeled (a) and (b) in Table II. The following conclusions can be drawn from the table: (1) there is no statistical significance to differences between the point source value and the line source values. (2) There is no statistical significance between the two line source values indicating good measurement reproducibility. Furthermore, we found no statistically significant difference between values computed from $\ln|T(z)|$ and values computed from $\varphi(z)$. This implies that losses to the surroundings, such as radiation loss, are negligible at the measurement frequencies (i.e., $h=0$). Also shown on the table are values of thermal conductivity calculated for each of the specimens. The calculation was based on averaging the three values of thermal diffusivity from the table and the values $\rho=3.515\ g\ cm^{-3}$ [Ref. 21] and $C=0.516\ J\ g^{-1}\ K^{-1}$ [Ref. 23].

Because the point source gives essentially the same result as the line source, an outcome consistent with the exact theory given in the appendix, it is preferable to use a point source when performing measurements on long bars. Larger signals were obtainable with a point heating source because more power could be put into the specimen. Furthermore, focusing the heating spot on the specimen is simpler with a spherical lens than with a cylindrical lens and alignment of the infrared optics is simpler with point heating.

Figure 3 shows a composite plot of all line source data and all point source data obtained from specimen LB-T. The data have been normalized by dividing by the square root of the modulation frequency. Equation (1) predicts a universal curve for $\varphi(z)/\sqrt{f}$ and a series of parallel curves for $\ln|T(z)|/\sqrt{f}$ which is essentially what we observe. The close coincidence of the phase data and the parallelism of all of the magnitude data away from the source (away from $z=0$) indicates that the one dimensional treatment in the infinite bar limit represents a good model for fitting the data. In the phase, the small differences observed near the origin are due to differences in data from the line source and data from the point source. These differences are attributed to the different source geometries. A similar argument holds for the differences in slopes of the magnitude data near the origin. These differences decrease as the distance from the source increases, as expected.

Table III lists μ for each specimen at each frequency. An important test for the validity of Eq. (1) depends on the relationship of μ to d,w, and the distance of the data used in the computation from a specimen end. Let us consider each case individually.

Above we stated that the condition $d \ll \mu$ should hold for Eq. (1) to provide an adequate description of the data. A comparison of values for d in Table I with values for μ in

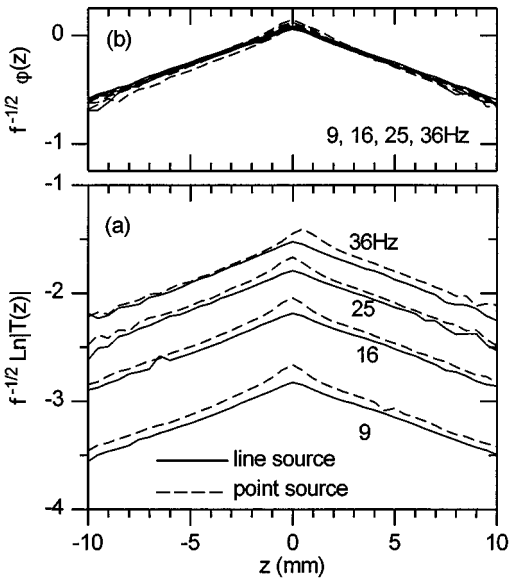

FIG. 3. A composite plots of all data obtained from specimen LB-T with both the line source and the point source. Plotted are (a) the logarithm of the signal magnitude divided by the square root of the modulation frequency vs detector position and (b) the phase of the signal divided by the square root of the modulation frequency vs detector position.

TABLE III. Thermal diffusion lengths,[a] μ (mm).

Frequency (Hz)	Specimen LB-E	Specimen LB-T	Specimen LB-X
9	2.8±0.1	4.8±0.2	5.4±0.3
16	2.1±0.1	3.6±0.2	3.9±0.2
25	1.7±0.1	2.9±0.1	3.2±0.1
36	1.4±0.1	2.4±0.1	2.6±0.1

[a]All combined standard uncertainties (±) are attributed principally to measurement repeatability and thus are taken to be one standard deviation of a measurement.

Table III indicates that this condition is adequately satisfied in all cases.

We find the relationship $w/2=2\ \text{mm}\ll\mu$ is not fulfilled. However, this represents a sufficient condition for using Eq. (1) but it is not a necessary condition. Experimentally we find that $2\ \text{mm}<\mu$ in all cases except for specimen LB-E at frequencies 25 and 36 Hz in which $2\ \text{mm}>\mu$. If the original condition were a requirement, we should find that D would depend on frequency. In fact, we find that the data follow a linear behavior sufficiently far (4 mm) from the source and D does not show any significant frequency dependence. The most severe test of this condition is the case of the point source. The data as seen in Fig. 3 reveal a nonlinear z dependence of the thermal signals in the immediate vicinity of the heating source. However, at a small distance from the heating source, the data become linear. In the case of line heating, we find that the region of linear signal behavior comes much closer to the heat source.

The distance from an end of the specimen should be at least 1.5 μ in order for interference by thermal wave reflections to be ignored. This condition also implies that there must be a minimum specimen length if Eq. (1) is to be applicable. Since the specimen is being heated at the center, the length of the specimen should be greater than 3 μ to take into account both ends plus an allowance for the heat source, in our case 4 mm to each side of the source, for a total of $3\mu+8$ mm. Using the values of μ for 9 Hz from Table III, we see that LB-X should be more than 24 mm long, LB-T should be more 23 mm long, and LB-E should be more than 17 mm long. In all cases, the length of the specimen is much greater than the minimum required length. In the appendix, we show that indeed, the linear behavior observed is to be expected in all cases if the distance from the heated spot is greater than 4 mm.

In order to show the effect of thermal wave reflection from the end of the specimen, we plot in Fig. 4 $\ln|T(z)|$ and $\varphi(z)$ vs z to one end of specimen LB-T ($f=5$ Hz, $\mu=6.6$ mm). Data obtained at 5 Hz are presented because the increased thermal diffusion length at this lower frequency enhances the end effect. The solid curves shown on the figure are obtained from the theoretical expression for a specimen of finite length,

$$T(z)=\frac{qe^{\pi/4}i}{2\sqrt{\omega\kappa\rho C}}\left[\frac{e^{\frac{|z|-L}{\mu}-\frac{|z|-L}{\mu}i}+e^{\frac{-|z|-L}{\mu}+\frac{|z|-L}{\mu}i}}{e^{\frac{L}{\mu}-\frac{L}{\mu}i}-e^{\frac{-L}{\mu}+\frac{L}{\mu}i}}\right], \tag{3}$$

where L is the distance from the center of the heating source to the end of the specimen ($L=26.5$ mm in this case); a

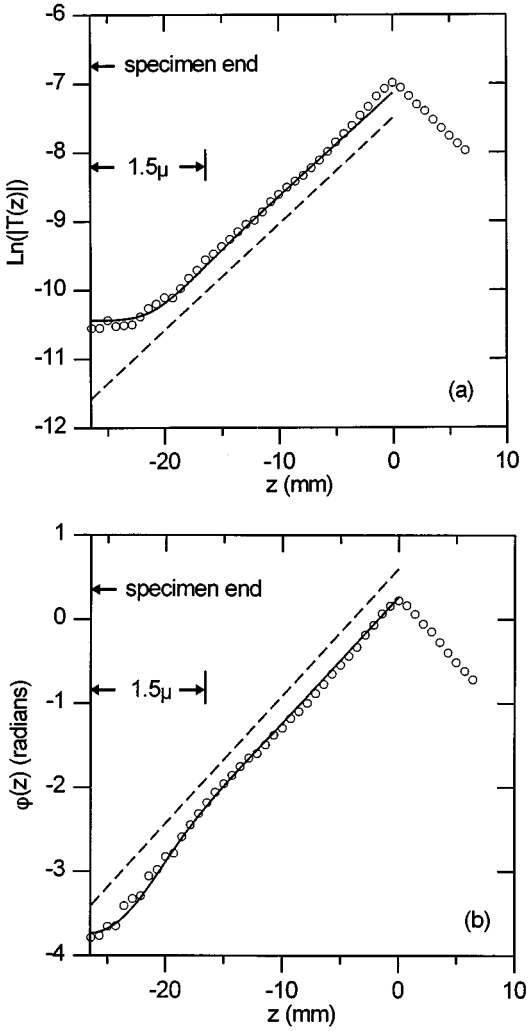

FIG. 4. Thermal wave signals for specimen LB-T as a function of detector position showing end effects. $f=5$ Hz, $\mu=6.6$ mm, $L=26.5$ mm. Superimposed on the data are plots based on the one dimensional theory. The dashed curves are straight lines that neglect the presence of the end; the solid lines take into account the end effects. The theoretical plots are not fits but were calculated from the thermal diffusivity value deduced in the prior measurements. Also indicated with arrows are one end of the specimen and the distance from the end equal to 1.5 times the thermal diffusion length, 1.5 μ. (a) Logarithm of the magnitude vs detector position, z. (b) Phase vs detector position, z.

fitting procedure was not used but the curves were adjusted visually which is equivalent to multiplying q by an arbitrary constant and adding an arbitrary constant to the phase. The theory predicts that the slope of both $\ln|T(z)|$ and $\varphi(z)$ will become zero at the specimen end, as can be seen in the figure. For comparison, we show the solution for the infinitely long specimen, which is represented by the dashed straight lines; here again the curves were similarly adjusted.

Our measurements have been made on a set of specimens that had been part of an interlaboratory round-robin comparison.[16] In Fig. 5, we compare our data with data obtained by three other laboratories that had used Hatta's modification of Ångström's method;[13] we did not include the other data because the methods used to obtain the data did not sample the thermal conductivity of the specimens in the same manner. Each reported value is represented by a solid

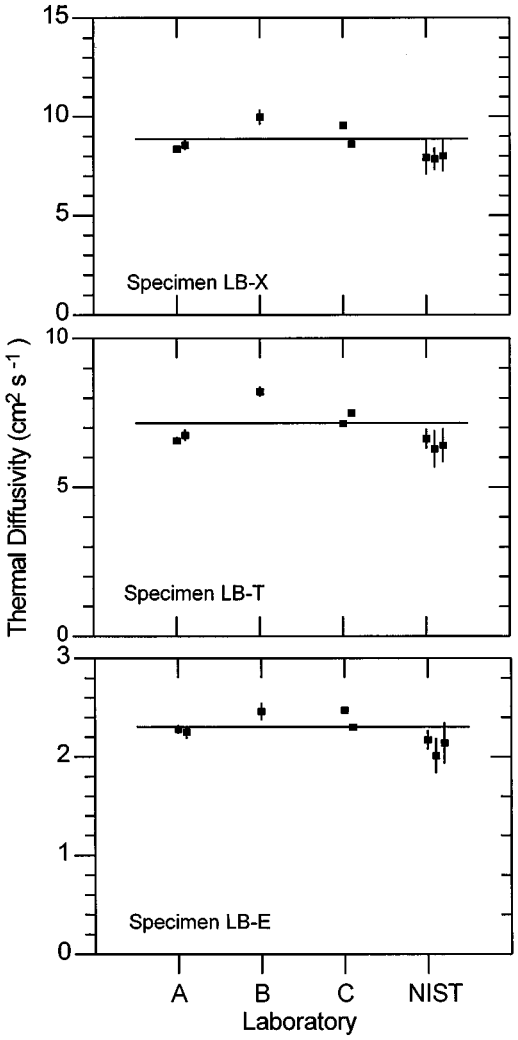

FIG. 5. A comparison of the values of thermal diffusivity we have obtained with the values obtained by three other laboratories. The horizontal line represents the average of the mean values of each laboratory and the vertical lines represent the error bars stated by each laboratory. In our case, an error bar represents one standard deviation. (See Table II.)

square and the uncertainty by a vertical line through the square; in the case of our measurements (the NIST data), the uncertainty represents one standard deviation of a measurement. The horizontal line on the graph represents the average of the mean values obtained by each laboratory.

All of the NIST values fall a little below the mean by an amount about equal to the measured uncertainties. This can be considered reasonably good agreement; our results agree best with the results of laboratory A. The uncertainties claimed by all of the other laboratories are much smaller than the NIST uncertainty yet they do not overlap with each other. The small uncertainty suggests that the precision of their measurements is high, yet the lack of overlap of the uncertainties suggests an unknown systematic difference. One source of the discrepancy may be different measurement temperatures at the different laboratories. Laboratory A and C report a measurement temperature of 25 °C while laboratory B reports a measurement temperature of 29 °C. It was not stated how these temperatures were measured.

ACKNOWLEDGMENTS

The authors thank Norton Diamond Film, General Electric, and Raytheon for providing the specimens. N. M. Balzaretti would like to thank the Brazilian National Council CNPq(Brazil) for personal financial support and the Universidade Federal do Rio Grande do Sul for the postdoctoral allowance.

APPENDIX

The purpose of this appendix is to demonstrate that the one dimensional solution is applicable under all of the experimental conditions described in this article.

The specimen consists of a long thin strip of width w and thickness d. Let x be the coordinate axis across the specimen width, where $x=0$ bisects the specimen; let y be the coordinate axis through the thickness, where $y=0$ is located on the specimen top surface; let z be the coordinate axis along the specimen length. The specimen is heated by a modulated source of angular frequency ω and having a spatial distribution $q(x,y)$ on a plane located at the specimen center, $z=0$. In this case, the complex solution to the heat diffusion equation is given by

$$T(x,y,z)=\frac{1}{2\kappa}\sum_{n=0}^{\infty}\sum_{m=0}^{\infty}q_{nm}\cos\left(\frac{2n\pi x}{w}\right)\cos\left(\frac{m\pi y}{d}\right)\times\frac{\exp\left(-|z|\sqrt{\left(\frac{2n\pi}{w}\right)^2+\left(\frac{m\pi}{d}\right)^2-\frac{2i}{\mu^2}}\right)}{\sqrt{\left(\frac{2n\pi}{w}\right)^2+\left(\frac{m\pi}{d}\right)^2-\frac{2i}{\mu^2}}},\tag{A1}$$

where q_{nm} is the nmth coefficient in the two dimensional Fourier series expansion of the heating source

$$q(x,y)=\sum_{n=0}^{\infty}\sum_{m=0}^{\infty}q_{nm}\cos\left(\frac{2n\pi x}{w}\right)\cos\left(\frac{m\pi y}{d}\right),\tag{A2}$$

and where we have assumed that the heating takes place on the top surface of the specimen, $y=0$, and is symmetrical about $x=0$. Furthermore, we have assumed no heat loss from the edges or surfaces of the specimen. Notice that the $\{n=0,m=0\}$ term in Eq. (A1) is the one dimensional solution.

In the following discussion, we consider only those terms with $m=0$. This is because the terms containing m and n have the same form and therefore will exhibit analogous behavior. Because $d\ll\mu$ in the case treated, we discuss below why terms with $m>0$ need not be considered at all.

Let us examine how each of the first three Fourier coefficients inside the summation in Eq. (A1) varies with z, where we assume $q_{n0}=1$ for all values of n. In our calculation, we have chosen $w=4$ mm and $\mu=1.4$ mm. This gives the smallest ratio reported in this article for $2\mu/w$, 0.7; if use of the one dimensional equation is valid in this case, then use of the one dimensional equation would be valid in all of the other cases. Figure 6 shows the dependence on z of the first three Fourier coefficients. All Fourier coefficients, including the higher order coefficients not shown, depend exponentially on z with the decay constant increasing dramatically

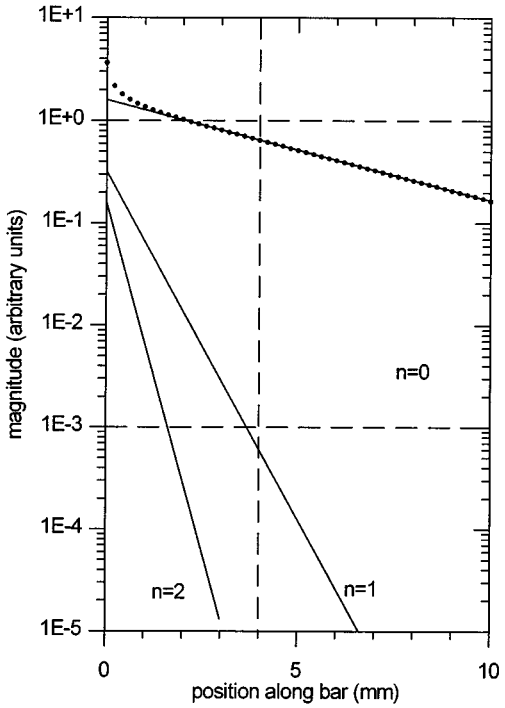

FIG. 6. Semilogarithmic plots of the magnitude of the complex temperature as a function of z along the central axis of the specimen ($x=0$). The parameters used in the computation were $x_0=0.044$, $w=4$, and $\mu=1.4$ mm. The solid curves represent each of the first three Fourier components of the temperature ($n=0,1,2$) assuming $q_{n0}/2\kappa=1$ for all n. The dotted curve represents the composite temperature obtained by summing on n ($m=0$), taking into account the relative strengths of the Fourier components of the heating beam. The vertical dashed curved corresponds to $z=4$ mm, a distance beyond which the one dimensional solution is clearly seen to be valid. The horizontal dashed lines are spaced by a factor of 10^3 in the magnitude.

with an increase in n (and m). Observe that for $x>4$ mm, the first order coefficient is less than a factor of 10^{-3} smaller than the zeroth order coefficient and all higher order coefficients are much smaller and therefore may be neglected, provided that $q_{n0}<\approx q_{00}$.

In our experiments, we employ a laser with an approximately Gaussian power profile, $\exp(-x^2/x_0^2)$, where $x_0=0.044$ mm. Let us calculate the ratio, q_{00}/q_{10}. The largest ratio occurs when the spot size is small, that is, $x_0 \ll w$. In this case, $q_{10}\approx 2q_{00}$, a result that has a minor effect on the relationship between the zeroth and first order terms in Eq. (A1). Thus, when $x>4$ mm, it is evident that the zeroth order term dominates completely, and the one dimensional treatment is applicable as stated in the manuscript. This is further demonstrated in Fig. 6 by the dotted curve which is the computed temperature magnitude normalized with respect to q_{00} and 2κ. The curve cannot be distinguished from the zeroth order curve even for values of $x<4$.

Equation (A1) demonstrates that the decay constants of the Fourier coefficients of the temperature increase with n and m; thus, the one dimensional term $\{n=0,m=0\}$ will always dominate provided that the distance from the heat source is sufficiently large. This distance will depend on the ratios $2\mu/w$ and μ/d. There is an inverse relationship between these ratios and the distance required for the one dimensional term to dominate.

In the case treated, $2\mu/w=0.7$ and $\mu/d=4.67$ ($d=0.3$ mm). We can now justify ignoring terms with $m>0$. If m were to be $\geqslant 1$, the decay constants would be much greater than those discussed above. If the specimen is partially or totally opaque, the degree of opacity will determine the relative size of Fourier components having different values of m. Since the term with $m=0$ is the only important one, the heat flow will be one dimensional regardless of the degree of opacity.

In real experiments, the source will also extend along the z axis. In this case, $q_{\rm nm}$ will be a function of z. If we replace $|z|$ by $|z-z'|$ in Eq. (A1), where z' is the source coordinate, we obtain the Green's function[24] representing a planar source. A source distributed along z will not affect our general conclusions; however, the position at which the one dimensional solution begins to dominate will shift by an amount determined by the spatial extent of the source along the z axis. In the case of Gaussian shaped source, the shift will be several times the width of the heating beam.

[1] P. E. Nordal and S. O. Kanstad, Phys. Scr. **20**, 659 (1979); S. O. Kanstad and P. E. Nordal, Can. J. Phys. **64**, 1155 (1986).
[2] M. A. Ångström, Philos. Mag. **25**, 130 (1863); Ann. Phys. (Leipzig) **114**, 513 (1861).
[3] P. Cielo, L. A. Utracki, and M. Lamontagne, Can. J. Phys. **64**, 1172 (1986).
[4] H. P. R. Frederikse and X. T. Ying, Appl. Opt. **27**, 4672 (1988).
[5] H. P. R. Frederikse, A. Feldman, and R. Fields, J. Appl. Phys. **72**, 2879 (1992).
[6] L. Fabbri and P. Fenici, Rev. Sci. Instrum. **66**, 3593 (1995).
[7] A. C. Bento and D. P. Almond, Meas. Sci. Technol. **6**, 1022 (1995).
[8] A. Feldman, H. P. R. Frederikse, and S. J. Norton, *Diamond Optics III*, edited by A. Feldman and S. Holly (SPIE, Bellingham, WA, 1990), Vol. 1325, pp. 304–314.
[9] G. Lu and W. T. Swann, Appl. Phys. Lett. **59**, 1556 (1991).
[10] J. E. Graebner, S. Jin, G. W. Kammlott, J. A. Herb, and C. F. Gardinier, Nature (London) **359**, 401 (1992).
[11] E. P. Visser, E. H. Versteegen, and W. P. van Enckevort, J. Appl. Phys. **71**, 3238 (1992).
[12] Z. Chen and A. Mandelis, Phys. Rev. B **46**, 13 526 (1992).
[13] I. Hatta, Y. Sasuga, R. Kato, and A. Maesono, Rev. Sci. Instrum. **56**, 1643 (1985).
[14] Y. Gu and I. Hatta, Jpn. J. Appl. Phys., Part 1 **30**, 1137 (1991); Y. Gu and L. Yu, Diam. Films Technol. **6**, 23 (1996).
[15] H. Altmann, O. Nilsson, and J. Fricke, in *Thermal Conductivity 23*, edited by K. E. Wilkes, R. B. Dinwiddie, and R. S. Graves (Technomic, Lancaster, PA, 1966), pp. 152–161.
[16] A. Feldman, ''Round Robin Thermal Conductivity Measurements on CVD Diamond'' in NIST Special Publication 885, *Applications of Diamond Films and Related Materials: Third International Conference*, edited by A. Feldman, M. Yoshikawa, Y. Tzeng, and M. Murakawa (U.S. GPO, Washington, DC, 1995), pp. 627–630.
[17] I. Hatta, R. Kato, and A. Maesono, Jpn. J. Appl. Phys., Part 1 **26**, 475 (1987).
[18] *Thermal Conductivity of Solids*, edited by J. E. Parrott and A. D. Stuckes (Pion, London, 1975), p. 24; B. Abeles, G. D. Cody, and D. S. Beers, J. Appl. Phys. **31**, 1585 (1960).
[19] M. B. Salamon, P. R. Garnier, B. Golding, and E. Buehler, J. Phys. Chem. Ref. Data Suppl. **35**, 851 (1974).
[20] D. P. Almond, P. M. Patel, I. M. Pickup, and H. Reiter, NDT&E Int. **18**, 17 (1985).
[21] B. N. Taylor and C. E. Kuyatt, *NIST Technical Note 1297*, 1994 ed. (U.S. GPO, Washington, DC, 1994).
[22] *The Properties of Diamond*, edited by J. E. Field (Academic, London, 1979), p. 643.
[23] *Physics Vade Mecum*, edited by H. E. Anderson (American Institute of Physics, New York, 1981), p. 323.
[24] A. Mandelis, J. Appl. Phys. **78**, 647 (1995).